Exactly solvable models of adaptive networks

Olivier Rivoire[1] and Julien Barré[2]

[1] *Laboratory of Living Matter, The Rockefeller University, 1230 York Ave., New York, NY-10021, USA.*
[2] *Laboratoire J. A. Dieudonné, Université de Nice-Sophia Antipolis, Parc Valrose, F-06108 Nice Cedex 02, France.*

(Dated: February 6, 2008)

A satisfiability (SAT-UNSAT) transition takes place for many optimization problems when the number of constraints, graphically represented by links between variables nodes, is brought above some threshold. If the network of constraints is allowed to adapt by redistributing its links, the SAT-UNSAT transition may be delayed and preceded by an intermediate phase where the structure self-organizes to satisfy the constraints. We present an analytic approach, based on the recently introduced cavity method for large deviations, which exactly describes the two phase transitions delimiting this adaptive intermediate phase. We give explicit results for random bond models subject to the connectivity or rigidity percolation transitions, and compare them with numerical simulations.

PACS numbers: 02.10.Ox,05.65.+b,05.70.Fh,75.10.Nr

Unraveling the principles responsible for the structure of observed technological, sociological or biological networks is currently an intensively pursued challenge [1]. Phase transitions occurring when the structure evolves are of particular interest. The simplest example is connectivity percolation, which takes place when the number of links increases [2]. Analogous phase transitions are found in constraint satisfaction problems (CSP's) defined on random graphs, such as the K-SAT or coloring problems [3]. They are referred to as SAT-UNSAT transitions and are related to the algorithmic complexity of solving these hard combinatorial problems [4].

While past studies of SAT-UNSAT transitions have confined to random distributions of constraints [5, 6], it has recently been suggested that an additional phase transition could arise if the network is allowed to respond to the addition of constraints by reorganizing itself [7, 8]. In this scenario, an adaptive intermediate phase (AIP) is predicted where the system avoids the SAT-UNSAT transition and adopts a structure distinct from random graphs. In this letter, we consider models whose configuration space consists of an ensemble of graphs, with a CSP defined on each graph, and we investigate the presence of an AIP by solving these models analytically with the cavity method for large deviations [9]. We thus provide one of the very few analytical results available for exponential random graphs models, the general class of networks to which our models belong (see e.g. [1]).

We apply our general approach to rigidity percolation on random bond models; this is a family of CSP's initially designed to model network glasses, the physical system for which the presence of an AIP was first suggested [7] and experimentally investigated [10]. In the absence of adaptation, these materials are expected to undergo a rigidity transition when the mean coordination of their atoms is varied by modifying their composition [11, 12]. As recalled below, this rigidity percolation can be viewed as a particular example of SAT-UNSAT transition [13]. Random bond models include models with a continuous connectivity percolation transition or a discontinuous rigidity percolation transition, which allows us to illustrate the necessity of a discontinuous SAT-UNSAT transition for observing an AIP. For rigidity percolation, we analytically describe this AIP and the related phase transitions by deriving new and presumably exact formulæ for large deviation functions.

Random bond models — Random bond models [14] are constructed from N point-like particles with d degrees of freedom each, by adding successively and at random bonds between them. Each bond carries only a bond-stretching constraint, so that the addition of a bond can have two effects: if the distance between its two end-points is already constrained, the new bond does not modify the total number of degrees of freedom and is considered as redundant; in the opposite case, it suppresses the degree of freedom associated with the relative distance between the two end-points. Globally, the number of independent internal degrees of freedom, or floppy modes, can be written

$$\mathcal{N}_{\text{floppy}} = dN - M + E_r - d(d+1)/2, \qquad (1)$$

where dN represents the total number of degrees of freedom, M the number of bonds, E_r the number of redundant constraints, and where $d(d+1)/2$ accounts for the global degrees of freedom in d dimensions.

In the thermodynamical limit where $N \to \infty$ and $M \to \infty$ with fixed ratio $\alpha = M/N$, the structure is a random graph with Poisson degree distribution [15], and the density of floppy modes, $n_f \equiv \mathcal{N}_{\text{floppy}}/N$, satisfies

$$n_f = d - \alpha + \epsilon_r, \qquad (2)$$

with $\epsilon_r \equiv E_r/N$. Two different phase transitions may occur when α is increased: rigidity percolation, when the largest rigid subgraph, with no floppy mode, becomes extensive; unstressed to stressed transition, when the

largest stressed subgraph, with a non-zero density of redundant constraints, becomes extensive. With random bonds, the two transitions occur in fact simultaneously at a critical value α_c [16].

An elementary counting argument, due to Maxwell [17], approximatively locates α_c by balancing the total number of constraints M with the total number of degrees of freedom, dN, yielding $\alpha_{\rm Mxl} = d$. The underlying assumption is that no redundant bond appears ($\epsilon_r = 0$) before the number of floppy modes vanishes ($n_f = 0$), which is not the case with random networks where the density of floppy modes never reaches zero (therefore $\alpha_c < \alpha_{\rm Mxl}$).

Constraint satisfaction — Random bond models can be recasted in the broader framework of CSP's as follows [13]. An instance of the problem is given by a graph G. An arrow is assigned to each link of G, which must point toward one of the two adjacent sites, and the set of different orientations defines the set of admissible solutions. Such a configuration σ is labeled by associating to each oriented link $i \to j$ a Boolean variable $\sigma_{i\to j} \in \{0, 1\}$ with $\sigma_{i\to j} = 1$ if the arrow is directed from i to j (and $\sigma_{j\to i} = 1 - \sigma_{i\to j}$). The cost function is

$$\mathcal{C}_G[\sigma] = \sum_i [\max(0, d - \sum_{j\in i} \sigma_{j\to i}) - (d - \alpha)] \qquad (3)$$

where $j \in i$ indicates that j is connected to i. Physically, an arrow means that the bond suppresses one degree of freedom to the node to which it points. By minimizing the cost function, we get the number of redundant constraints for the graph G [13]:

$$E_r[G] = \min_\sigma \mathcal{C}_G[\sigma]. \qquad (4)$$

Note that $\mathcal{C}_G[\sigma] \geq 0$ for any σ, so that $E_r[G] \geq 0$ as it should. We will focus on two particular cases: $d = 2$ which describes $2d$ rigidity percolation, and $d = 1$, which describes the usual connectivity percolation.

Infinite temperature transition — The formulation in terms of CSP allows to resort to the cavity method [18] to determine the phase diagram as a function of the density of constraints α, when G is taken at random from the ensemble $\mathcal{G}_N^{(\alpha)}$ of graphs with N nodes and $M = \alpha N$ links [13]. This method indeed applies to any CSP defined on such random graphs, and has notably lead to the derivation of the phase diagrams of the K-SAT and coloring problems [5, 6]. In contrast with these algorithmically hard CSP's, the present model can be solved by the simplest, "replica symmetric" [19], formulation of the cavity method. The density of redundant constraints thus obtained is consistent with previous studies [20] and reads

$$\epsilon_r = \sum_{k=d+1}^{\infty} \pi_{2\alpha\eta}(k) \left(\frac{k}{2} - d\right), \quad \eta = \sum_{k=d}^{\infty} \pi_{2\alpha\eta}(k), \qquad (5)$$

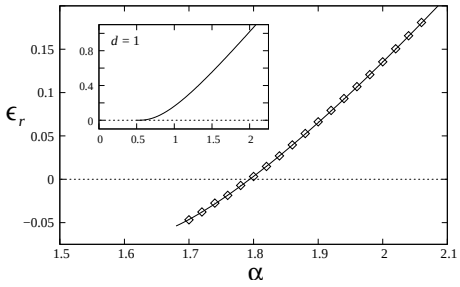

FIG. 1: Density of redundant constraints ϵ_r for $d = 2$ as calculated from Eqs. (5); the symbols are from numerical simulations confirming that the negative part corresponds to the number of floppy modes on the 3-core. Inset: ϵ_r for $d = 1$.

where $\pi_\theta(k) = e^{-\theta}\theta^k/k!$. A non-zero solution, $\eta > 0$, exists only for $\alpha > \alpha_p^{(d)}$. This threshold corresponds to the percolation of the $(d + 1)$-core [20], that is, the emergence of a sub-graph containing an extensive number of nodes all having connectivity at least $(d+1)$ [15] (only the percolation of the 2-core occurs simultaneously with connectivity percolation [15]). As shown in Fig. 1, for $d \geq 2$, when this non-zero solution appears, the corresponding ϵ_r is negative, and becomes positive only at $\alpha_c^{(d)} > \alpha_p^{(d)}$.

Such a negative prediction for an intrinsically positive quantity is often indicative of the inadequacy of the replica symmetric assumption [5, 6]. For the present problem however, we verified that no replica symmetry breaking could occur and found instead a simple interpretation for the calculated $\epsilon_r < 0$: Eqs. (5) correspond to Maxwell counting on the $(d+1)$-core. While Maxwell argument is only approximate for the complete graph, we propose that it is exact on the $(d+1)$-core, with the onset of stressed nodes coinciding with the disappearance of floppy modes; in other words, ϵ_r gives the number of floppy modes on the $(d + 1)$-core when negative, and the number of redundant constraints when positive. We verified numerically this interpretation using the Pebble Game algorithm [21], see Fig. 1.

It follows that the rigidity percolation on the complete graph occurs not at the $(d + 1)$-core percolation threshold $\alpha_p^{(d)}$ but at the point $\alpha_c^{(d)}$ where ϵ_r becomes positive (for $d = 1$, the two thresholds coincide). The same conclusion was reached in earlier studies [16, 20], based on comparison with numerical simulations.

Finite temperature — To analyze the consequences of allowing the network of constraints to adapt, we now consider the system whose configuration space is the ensemble $\mathcal{G}_N^{(\alpha)}$ of graphs with N nodes and $M = \alpha N$ links. To each graph $G \in \mathcal{G}_N^{(\alpha)}$, we associate as energy the number $E_r[G]$ of redundant constraints, as given by Eq. (4). The partition function is thus $\mathcal{Z}_N(y) = \sum_{G\in\mathcal{G}_N^{(\alpha)}} e^{-yE_r[G]}$ where the inverse temperature y allows to sample different subsets of $\mathcal{G}_N^{(\alpha)}$, with the infinite temperature limit $y = 0$ corresponding to selecting the graphs irrespectively

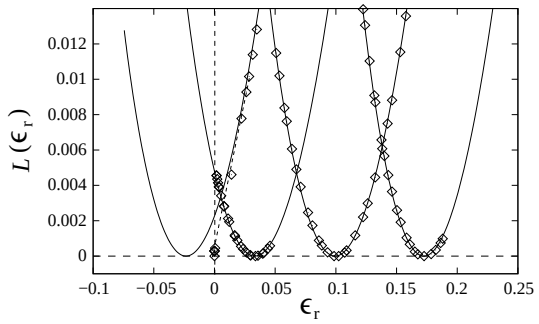

FIG. 2: Rate functions $L_{\rm cav}(\epsilon_r)$ with $d = 2$ and $\alpha = 1.75$, 1.85, 1.95 and 2.05 (from left to right at the bottom), as obtained from Eqs. (8). The symbols are results of Monte Carlo simulations at fixed y. For $\alpha < \alpha^{(2)}_{\rm Mxl}$], the branches with $\epsilon_r < 0$ must be replaced by $L(\epsilon_r < 0) = \infty$. For $\alpha = 1.75 < \alpha_c^{(2)}$, a part of the curve with $\epsilon_r > 0$ must also be substituted by a Maxwell construction (dotted line).

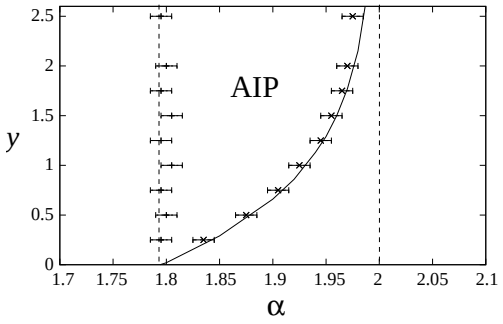

FIG. 3: Phase diagram for $d = 2$. The two vertical dashed lines are for $\alpha_c^{(2)} = \alpha_c^{(2)}(0)$ and $\alpha^{(2)}_{\rm Mxl} = 2$, and the full line is for $\alpha_c^{(2)}(y)$. At any fixed $y > 0$, an intermediate phase is present between $\alpha_c^{(2)}(0)$ and $\alpha_c^{(2)}(y)$. The symbols are numerical estimates for the locations of the two phase transitions.

of their energy, as considered previously. $\mathcal{Z}_N(y)$ can be evaluated by computing the microcanonical entropy density $s(\epsilon_r)$ which gives through $\exp[Ns(\epsilon_r)]$ the number of graphs in $\mathcal{G}_N^{(\alpha)}$ with density of redundant constraints ϵ_r. An equivalent information is contained in the rate function $L(\epsilon_r)$, defined from the probability $\mathbb{P}_N(\epsilon_r)$ for a graph in $\mathcal{G}_N^{(\alpha)}$ to have density of constraints ϵ_r; indeed, if $\mathbb{P}_N(\epsilon_r)$ satisfies a large deviation principle, $\mathbb{P}_N(\epsilon_r) \asymp \exp[-NL(\epsilon_r)]$ ($a_N \asymp b_N$ means that $\ln a_N / \ln b_N \to 1$ as $N \to \infty$), and, if $|\mathcal{G}_N^{(\alpha)}|$ denotes the number of graphs in $\mathcal{G}_N^{(\alpha)}$, we have $\exp[Ns(\epsilon_r)] = |\mathcal{G}_N^{(\alpha)}| \exp[-NL(\epsilon_r)]$. The equilibrium properties of the system are thus captured by the potential $\phi(y)$, with

$$e^{-N\phi(y)} = |\mathcal{G}_N^{(\alpha)}|^{-1} \mathcal{Z}_N(y) \asymp \int \mathrm{d}\epsilon_r \; e^{N[y\epsilon_r - L(\epsilon_r)]}, \quad (6)$$

from which by Legendre transform we get

$$\epsilon_r = \partial\phi(y)/\partial y, \qquad L(\epsilon_r) = -y\epsilon_r + \phi(y). \quad (7)$$

This potential can be computed by the large deviation cavity method [9], an extension of the cavity method to atypical graphs. For random bond models, it yields:

$$\begin{aligned} \phi(y) &= -\ln Z + 2\alpha \left[1 - (1-\eta)e^y e^{-z}\right] - \alpha z, \\ Z &= e^{2\alpha\eta e^{-z}} + \sum_{r=0}^{d-1} \pi_{2\alpha\eta e^{-z}}(k) \left(e^{-y(d-k)} - 1\right), \\ z &= \ln\left[e^y + (1-e^y)\eta^2\right], \\ \eta &= 1 - \frac{1}{Z} \sum_{k=0}^{d-1} \pi_{2\alpha\eta e^{-z}}(k) e^{-y(d-k)}. \end{aligned} \quad (8)$$

Examples of rate functions $L_{\rm cav}(\epsilon_r)$ obtained from the non-trivial solution ($\eta > 0$) of these equations are displayed in Fig. 2 for $d = 2$ and four representative values of α; they are perfectly consistent with numerical results. For $\alpha < \alpha^{(2)}_{\rm Mxl} = 2$, $L_{\rm cav}(\epsilon_r)$ extends to $\epsilon_r < 0$. As we checked with numerical simulations, these unexpected negative values have the same interpretation as in the typical case ($y = 0$). This suggests that the correct rate function $L(\epsilon_r)$ is obtained from $L_{\rm cav}(\epsilon_r)$ by truncating the negative branch: $L(\epsilon_r) = L_{\rm cav}(\epsilon_r)$ if $\epsilon_r > 0$, and $L(\epsilon_r) = \infty$ if $\epsilon_r < 0$. For $d = 1$, where $L_{\rm cav}(\epsilon_r)$ never shows a negative branch, our formulæ coincide with rigorous results from the mathematical literature [22] (we are not aware of any previous result for $d \geq 2$).

Intermediate phase — The rate function $L(\epsilon_r)$ completely specifies the equilibrium properties of the system for any y. Geometrically, the relation $y = -\partial L(\epsilon_r)/\partial\epsilon_r$ indicates that $\epsilon_r(y)$ is the intersection of $L(\epsilon_r)$ with the supporting line having slope $-y$ (the line below $L(\epsilon_r)$ touching $L(\epsilon_r)$ in a single point). For $\alpha < \alpha_c^{(d)}$, we thus get $\epsilon_r(y) = 0$. For $\alpha > \alpha_c^{(d)}$, the rate function has a decreasing part whose slope, by convexity, is extremal at the lower edge, $\epsilon_r = 0$, with value denoted $y_c^{(d)}(\alpha) = -\partial L/\partial\epsilon_r(\epsilon_r = 0^+)$. If $y < y_c^{(d)}(\alpha)$, which is necessarily the case for $d = 1$ where $y_c^{(1)}(\alpha) = \infty$, the density of redundant constraints is $\epsilon_r(y) > 0$ and the system is in an UNSAT phase. For $d \geq 2$ however, since $y_c^{(d)}$ is finite when $\alpha_c^{(d)} < \alpha < \alpha^{(d)}_{\rm Mxl}$, there is an adaptive intermediate phase (AIP) between $\alpha_c^{(d)}$ where $y_c^{(d)}(\alpha) = 0$ and $\alpha_c^{(d)}(y)$ where $y_c^{(d)}(\alpha) = y$. In this phase, the system maintains itself at the edge of the SAT-UNSAT transition, with $\epsilon_r(y) = 0$. The resulting phase diagram is presented in Fig. 3 for $d = 2$.

The atypical, self-organized, nature of the graphs in the AIP can be quantified with $\rho = \sigma^2/(2\alpha)$, the ratio of the variance σ^2 of the degree distribution, over its mean 2α. Indeed, typical random graphs have a Poisson degree distribution [15], for which $\rho = 1$, and a value $\rho \neq 1$ is therefore indicative of atypical graphs. We computed ρ with the large deviation cavity method, and found, as shown in Fig. 4, that it presents two slope discontinu-

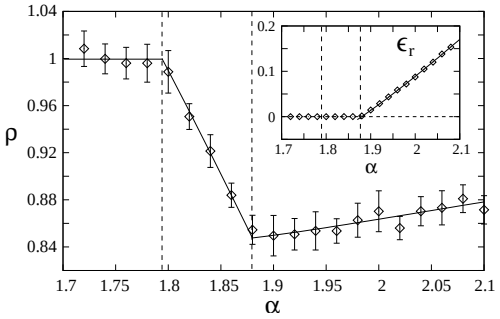

FIG. 4: Order parameter $\rho = \sigma^2/(2\alpha)$ for $d = 2$ when varying α at fixed $y = 0.5$. From the entry in the AIP at $\alpha_c^{(2)} = 1.79$, the networks are atypical (non-Poisson) random graphs with $\rho < 1$. The symbols with error bars are from Monte Carlo simulations. Inset: analytical and numerical results for $\epsilon_r(y)$.

ities, at the two boundaries of the AIP; the density of redundant constraints ϵ_r in contrast is strictly zero until α reaches $\alpha_c^{(d)}(y)$. This result is in very good agreement with our numerical simulations, and clearly demonstrates that the transition at $\alpha_c^{(d)}$ is of a different, topological, nature than the SAT-UNSAT transitions taking place here at $\alpha_c^{(d)}(y) > \alpha_c^{(d)} \equiv \alpha_c^{(d)}(y = 0)$.

Zero temperature — It is worth mentioning that the extreme case $y = \infty$, which has been the focus of several numerical studies [7, 23] appears here as a very singular limit. In this case indeed, the distinction made previously between $y_c^{(d)}$ being infinite or not is irrelevant since y itself is infinite. An asymptotic analysis of our solution reveals that when $y = \infty$ an AIP is present between $\alpha_c^{(d)}$ and $\alpha_{\rm Mxl}^{(d)}$ for any value of d, including $d = 1$ for which it disappears as soon as $y < \infty$. This suggests that in finite dimensional models, where the rigidity transition is thought to be continuous, the AIP could be confined to $y = \infty$. An AIP at finite y may be present only as cross-over, which could also account for the experimental observations in network glasses.

Discussion — CSP's such as K-SAT or coloring are known for displaying a clustered intermediate phase (CIP), also known as hard-SAT phase, where the set of solutions breaks into an exponential number of disconnected components [5, 6]. This CIP, which, in contrast to the AIP, takes place prior to the UNSAT-SAT transition, is however of a radically different character: it refers to a transition in the space of solutions associated to single, typical, graphs, and not to a transition in a graph space. We analyzed here random bond models, which we argued do not involve replica symmetry breaking, and thus have no CIP. CSP's with a CIP could however be tackled along the same lines to study the interplay between the two kinds of intermediate phases.

In conclusion, we presented a general analytical approach for solving the equilibrium thermodynamics of models of adaptive networks. This leads us to the exact description of a new kind of topological phase transition, which takes place in a configuration space made of graphs. Our findings confirm that the presence of a discontinuous SAT-UNSAT transition in the typical problem is essential for observing an adaptive intermediate phase (AIP) [8]. The principles behind the self-organization of graphs found in the AIP differ notably from most of the mechanisms proposed so far to explain the non-random structure of networks. Our model indeed belongs to the family of exponential random graphs, a still poorly understood class of networks [1]. Our results show that the cavity method for large deviations is a powerful tool to study at least some of these models.

Acknowledgments — We warmly thank Mykyta Chubynsky, for making available to us his implementation of the Pebble Game algorithm. O.R. is a fellow of the Human Frontier Science Program.

[1] M. E. J. Newman, SIAM Review **45**, 167 (2003).
[2] D. Staufler and A. Aharony, *Introduction to Percolation Theory* (Taylor and Francis, London, 1992).
[3] C. H. Papadimitriou and K. Steiglitz, *Combinatorial Optimization: Algorithms and Complexity* (Prentice Hall, Englewood Cliffs, NJ, 1982).
[4] R. Monasson, R. Zecchina, S. Kirkpatrick, B. Selman, and L. Troyansky, Nature **400**, 133 (1999).
[5] M. Mézard and R. Zecchina, Phys. Rev. E **66**, 056126 (2002).
[6] R. Mulet, A. Pagnani, M. Weigt, and R. Zecchina, Phys. Rev. Lett. **89**, 268701 (2002).
[7] M. F. Thorpe, D. J. Jacobs, M. V. Chubinsky, and J. C. Phillips, J. Non-Cryst. Solids **859**, 266 (2000).
[8] J. Barré, A. R. Bishop, T. Lookman, and A. Saxena, Phys. Rev. Lett. **94**, 208701 (2005).
[9] O. Rivoire, J. Stat. Mech. P07004 (2005).
[10] D. Selvanathan, W. J. Bresser, and P. Boolchand, Phys. Rev. B **61**, 15061 (2000).
[11] J. C. Phillips, J. Non-Cryst. Solids **34**, 153 (1979).
[12] M. F. Thorpe, J. Non-Cryst. Solids **57**, 355 (1983).
[13] J. Barré, A. R. Bishop, T. Lookman, and A. Saxena, J. Stat. Phys. **118**, 1057 (2005).
[14] P. Duxbury, D. Jacobs, M. Thorpe, and C. Moukarzel, Phys. Rev. E **59**, 2084 (1999).
[15] B. Bollobás, *Random graphs* (Cambridge University Press, 2001), 2nd ed.
[16] M. F. Thorpe, D. J. Jacobs, N. V. Chubynsky, and A. J. Rader (Kluwer Academic, New York, 1999), p. 239.
[17] J. C. Maxwell, Philos. Mag. **27**, 294 (1864).
[18] M. Mézard and G. Parisi, J. Stat. Phys. **111**, 1 (2003).
[19] M. Mézard, G. Parisi, and M. A. Virasoro, *Spin-Glass Theory and Beyond*, (World Scientific, Singapore, 1987).
[20] C. F. Moukarzel, Phys. Rev. E **68**, 056104 (2003).
[21] D. J. Jacobs and M. F. Thorpe, Phys. Rev. Lett. **75**, 4051 (1995).
[22] A. A. Puhalskii, Ann. Probab. **33**, 3374412 (2005).
[23] M. V. Chubynsky, M.-A. Brière, and N. Mousseau (2006), cond-mat/0602412.